Mechanical weakness of thoracic aorta related to aging or dissection predicted by speed-of-sound with collagenase

メタデータ	言語: eng
	出版者:
	公開日: 2022-01-26
	キーワード (Ja):
	キーワード (En):
	作成者: Miura, Katsutoshi, Yamashita, Kanna
	メールアドレス:
	所属:
URL	http://hdl.handle.net/10271/00003939

1 **Mechanical weakness of thoracic aorta related to aging or dissection predicted by**

2 **speed-of-sound with collagenase**

3

4 Katsutoshi Miura[a],[*] and Kanna Yamashita[a]

5

6 [a]Department of Health Science, Pathology and Anatomy, Hamamatsu University School

7 of Medicine, Hamamatsu, Japan

8

9 *Corresponding author

10 1-20-1 Handa-yama, Higashiku, Hamamatsu 431-3192, Japan

11 Tel: 81-53-435-2811

12 Fax: 81-53-435-2800

13 E-mail: kmiura@hama-med.ac.jp

14   **Abstract**

15   **Scanning acoustic microscopy reveals information about histology and**

16   **speed-of-sound (SOS) through tissues. Slower SOS corresponds to lower stiffness.**

17   **The present study aimed to investigate whether SOS values reflect the degree of**

18   **degeneration with aging or dissection and whether enzymatic digestion**

19   **susceptibility is distinct**. SOS of media besides the atheromatous areas of normal and

20   surgical dissections was measured and compared using medial degeneration grade

21   (MDG) scores. To evaluate the damage rate, SOS was assessed following collagenase

22   digestion. SOS scores negatively correlated with aging and MDG scores. Dissected

23   aortae showed higher SOS and MDG scores without age correlation. Collagenase

24   digestion was present in all aortae, but older aortae were more injured than younger

25   aortae. Dissected aortae were more vulnerable to collagenase. Older and dissected

26   aortae expressed specific extracellular matrix (ECM) components to compensate for

27   mechanical weakness. The present method can evaluate mechanical weakness

28   corresponding to histology to investigate the cause of rupture.

29

30   **Keywords**: scanning acoustic microscopy, collagenase, extracellular matrix, thoracic

31   aorta, medial degeneration grade, aging, dissected aorta

32

Introduction

Aortic diseases are a major health concern that may result in aneurysm, dissection, and atherosclerotic occlusion (Tsamis et al. 2013). A normally elastic aorta can begin to stiffen with age (Radu-Ionita et al. 2017). Losing elasticity due to conditions such as atherosclerosis or Marfan (MF) syndrome causes serious disorders.

The aortic wall media are organized into lamellar units, comprising concentric layers of elastic lamellae, smooth muscle cells, and interlamellar matrix (Brooke et al. 2003). Elastic fibers are predominantly composed of elastin, whereas the interlamellar matrix contains structural/supporting proteins, such as type-I collagen, type-III collagen, and fibrillin (FBN). All extracellular matrix (ECM) components provide structural organization and stability to the vessel wall through interactions between the smooth muscle cells and associated ECM elements. Moreover, these elements include lysyl oxidase (LOX), vitronectin (VN), and fibronectin (FN). Collagens bind and signal to smooth muscle cells through specific matrix receptors. Elastic fibers are linked to smooth muscle cells through a microfibril scaffold consisting of FBN and microfibril-associated glycoproteins.

All aortic diseases are associated with microstructural changes in the content or architecture of the connective fibers (Tsamis et al. 2013). Connective fibers consist of

51   elastin and collagen (Tsamis et al. 2013), which confer elasticity and strength to a

52   healthy aorta, respectively. Matrix metalloproteinases (MMPs), which include

53   collagenases, are a family of endopeptidases with proteolytic activity toward both

54   elastin and collagen (Choke et al. 2005). The high collagenase activity of the aorta

55   contributes to aneurysms and rupture (Menashi et al. 1987; Busuttil 1980). MMP-1

56   (collagenase-1), -8 (collagenase 2), and -13 (collagenase-3) are enzymes specific for

57   collagens. Collagenase-3 was used to imitate biochemical injury to aortae and detect

58   susceptibility to aneurysm and aortic rupture.

59   **The elasticity of the aortae has been reported in dogs (Hughes et al. 1979)**

60   **and humans (Sutton-Tyrrell et al. 2005; Lehmann et al. 1993) by measuring pulsed**

61   **wave velocity. Other methods to estimate aortic elasticity *in vivo* include**

62   **elastography (Fromageau et al. 2008) or micro-elastography (Schmitt et al. 2010),**

63   **which use shear waves, and 4D ultrasound (Wittek et al. 2013) which apply**

64   **time-resolved three dimensional ultrasound.**

65   These methods can provide macroscopic information about the elasticity of the

66   entire arterial wall, including the intima, media, and adventitia. However, they do not

67   address local tissue elements such as smooth muscle loss, accumulation of ECM

68   components, aneurysm, and dissection.

69   Scanning acoustic microscopy (SAM) can evaluate both histological and

70   viscoelastic properties (Mamou and Rohrbach 2017; Miura 2016; Saijo 2009).

71   Since Lemons and Quate (1974) at Stanford University provided the basic design

72   of SAM in the biomedical field, many studies have reported on biological objects at

73   low frequencies (ranging from 1 to 10 MHz) (Maev 2008). Studies of the acoustic

74   properties of tissues at low frequencies suggest that SOS in soft tissues differs only

75   slightly from its value in water and is virtually independent of frequency (Duck

76   1990). Only solid tissue, such as bones, and tissues rich in fibrillar proteins showed

77   significant differences. Many acoustic images were collected and analyzed by

78   Quate's team, primarily using fixed unstained tissues. Low-frequency studies (1 to

79   7 MHz) of acoustic parameters of tissues (attenuation coefficients, SOS) have

80   demonstrated that fixation in 4% formalin changes these parameters only slightly

81   (Bamber et al. 1979).

82   Studies of acoustic properties of biological tissues at high frequencies (>

83   100 MHz) have recently began to obtain high-resolution quantitative images.

84   Improvements such as transducers with a very small F-number and high

85   sensitivity (Mamou and Rohrbach 2017) and time-frequency analysis method

86   (Hozumi et al. 2004) have contributed to this progress. Even single cells can now be

87 **identified in the subcellular structures (Lemor et al. 2004; Weiss et al. 2007) and**

88 **clinical cytology samples (Miura and Yamamoto 2015).**

89   The speed-of-sound (SOS) of tissues observed using SAM is given as:

90
$$c = \sqrt{K/\rho},$$

91 where c is the SOS, K is the elastic bulk modulus, and ρ is the density.

92   This formula implies that the SOS strongly reflects its elastic parameter. SOS values

93 (m/sec)have been reported for many tissues (Azhari 2010; Saijo et al. 1998)**.** In general,

94 SOS has low values in fluid-filled soft structures and high values in dense solid tissues.

95 SOS values are well-correlated with the palpable tissue stiffness. Therefore, ultrasound,

96 *in vivo* imaging-based methods such as elastography (Mahmood et al. 2016), and *in*

97 *vitro* tests on isolated samples, such as the SAM method, are available for estimating

98 the mechanical properties of biological samples. The current study used a stored

99 collection of ascending aorta (AAo) surgical specimens with detailed clinical history,

100 including dissection episode, to investigate the elasticity of the specimen and observe

101 histology to gain etiological insights.

102   Aortic walls progressively lose their components and increase their content in

103 fibrous tissue, leading to greater stiffness with aging. Aging aortae can lead to two

104   conditions involving greater or thinner wall thickness (Tsamis et al. 2013). The first is

105   atherosclerosis, which causes wall thickening due to development of a fatty plaque. The

106   second is aneurysm, which is produced by balloon-like thinning of the wall due to local

107   weakness. Focal portions of aortae fail to compensate mechanical strength to form

108   aneurysm or second bleb in aneurysm. The specific etiology of dissection due to aging

109   or genetic defects is unknown to date (Wu et al. 2013).

110   The aim of the present study was to investigate whether SOS values reflect the

111   degree of aortic degeneration and whether resistance to collagenase digestion is

112   different between aged and dissected cases. Moreover, the biochemical changes in ECM

113   components were compared between aging aortae and dissected aortae.

114

115   **Materials and Methods**

116   ***Subjects and ethics***

117   All human tissue sections were obtained from samples stored in the tissue archives of

118   the Hamamatsu University Hospital or Shizuoka City Hospital in Japan. The AAo of

119   adult autopsied patients without serious cardiovascular diseases were consecutively

120   selected to investigate the effects of aging on the biomechanical properties of the aortae

121   (n = 36; age, 62.9 ± 20.0 years; 24 men and 12 women). Cases of MF syndrome (n = 7;

7

122   age, 46.7 ± 16.2 years; three men and four women) and non-MF syndrome (n = 9; age,

123   56.3 ± 12.0 years; seven men and two women) were selected from surgical specimens of

124   dissected AAo aneurysm with known clinical history. Formalin-fixed,

125   paraffin-embedded (FFPE) tissue blocks were flat-sectioned into 10-µm-thick slices and

126   observed using SAM. The research protocol for using stored samples without a link to

127   patient identity was approved by the Ethics Committee of Hamamatsu University

128   School of Medicine (No. 14-135, 19-180). Written consent was waived based on the

129   retrospective design. All procedures were conducted according to approved guidelines

130   and regulations.

131

132   *SAM observations*

133   **The experimental protocol is detailed in Fig. 1. Aortic tissue specimens were**

134   **evaluated using SAM system (AMS-50AI, Honda Electronics, Toyohashi, Aichi,**

135   **Japan) with a central frequency of 320 MHz, lateral resolution of 3.8 μm, and**

136   **thickness of the focal spot of 13 μm. A single-pulsed ultrasound with 2-ns pulse**

137   **width was emitted (Hozumi et al. 2004). Distilled water was used for coupling fluid**

138   **between the transducer and the specimen. The transducer was used for both**

139   **transmitting and receiving the signal. Reflected waveforms from the surface and**

140   the bottom of specimen were compared to measure the SOS and the thickness of

141   each point. Waveform from the glass surface without the specimen present was

142   used as a reference waveform.

143   Scanning the transducer over the specimen formed an acoustic image. The

144   mechanical scanner was arranged so that the ultrasonic beam was transmitted at

145   every 8, 4 and 2 μm interval over a 2.4, 1.2, and 0.6 mm width, respectively. The

146   number of sampling points was 300 in one scanning line, and 300 x 300 points

147   made one frame. Four pulse echo sequences were arranged for each scan point in

148   order to increase the signal-to-noise-ratio. Each pixel of an image corresponds to

149   an echo coming from an x-y position on the specimen.

150   The observed samples were prepared by cutting FFPE blocks. Although FFPE samples

151   have been demonstrated as having slightly higher SOS than fresh samples, the SOS

152   values were stable (Sasaki et al. 1996) irrespective of periods of formalin fixation from

153   1 day to 3 months (Miura et al. 2015). Therefore, sample bias due to fixation condition

154   was negligible. Areas without calcified deposits and heavy atheroma were selected for

155   comparison. **Calcified areas result in chatter marks on the section, which causes**

156   **irregular reflection and heavy atheromatous portions become translucent due to**

157   **lipid dissolution in organic solvents. In dissected cases, non-dissected portions**

158 **away from the separation were used for SOS measurement.**

159

160 *SOS difference according to age and disease status (normal, MF syndrome, and*

161 *non-MF syndrome)*

162 To evaluate age-related changes of the aorta, the average SOS values of the aortic media

163 were plotted according to age. To compare the mechanical weakness and structural

164 differences, the samples were divided into two groups: (1) younger adults aged 31–58

165 years (average, 46.7 ± 11.47 years; $n = 6$; four men and two women) and (2) older

166 individuals aged 76−85 years (average, 80.2 ± 3.42 years; $n = 5$; four men and one

167 woman). The SOS values of dissected aortae (including MF syndrome and non-MF

168 syndrome) ($n = 16$; age 52.1 ± 14.3 years; 10 men and 6 women) were also compared

169 with age-matched normal aortae ($n = 12$; age 56.8 ± 15.7 years; 8 men and 4 women) by

170 plotting the average SOS values of the aortic media according to age.

171

172 *Catalytic damage according to collagenase digestion*

173 Paraffin sections were dewaxed using xylene, soaked in distilled water, and submerged

174 into a solution of phosphate-buffered saline containing 0.5 mM $CaCl_2$ (pH 7.4) plus 250

175 units/mL type-III collagenase (Worthington, Lakewood, NJ, USA) at 37°C for 1.5 h or

176 twice for 1.5 h (Miura and Katoh 2016). According to the manufacturer's instructions,

177 type-III collagenase has typical collagenase activity but lower proteolytic activity than

178 other collagenases. SOS was measured both before (baseline) and after digestion.

179 Digested sections were first washed with distilled water before being analyzed with

180 SAM. The same sections were measured after a repeated digestion (two 1.5-h

181 treatments).

182

183 *Medial degeneration grade (MDG) evaluation*

184 To compare SAM with light microscopy (LM) images, the same or nearby sections were

185 stained with hematoxylin, eosin, and Elastica Masson trichrome (EMT) to stain collagen

186 and elastic fibers blue and black, respectively. The magnification of each LM image was

187 adjusted to match the corresponding SAM image with scale bars on the bottom and the

188 left side of the screen frame.

189 Consensus criteria was used to evaluate the extent and severity of the aortic

190 MDG scores (Halushka et al. 2016). These criteria included mucoid extracellular matrix

191 accumulation, elastic fiber fragmentation/loss, smooth muscle cell nuclei loss, and

192 laminar medial collapse. The overall MDG was scored as 0 (none), 1 (mild), 2

193 (moderate), or 3 (severe).

194

Immunohistochemical analysis

196 Immunostaining was performed using a commercially available Chemmate envision kit

197 (Dako, Glostrup, Denmark). The following primary antibodies used: anti-smooth

198 muscle actin (SMA) (ab5694, Abcam, Tokyo, Japan; 1:400), anti-collagen I (ab88147,

199 Abcam, 1:100) and anti-collagen III (ab7778, Abcam, 1:1000) for collagen types,

200 anti-LOX (ab174316, Abcam, 1:300), anti-VN (ab46808, Abcam, 1:250), anti-FBN

201 (ab53076, Abcam, 1:25), and anti-FN (ab2413, Abcam, 1:250). Heat-mediated antigen

202 (95°C, 20 min) was retrieved with buffer balanced to either pH 6.0 (anti-SMA,

203 anti-collagen III, FN) or pH 9.0 (anti-collagen I, anti-LOX, anti-VN) before staining.

204

Statistical analyses

206 The average SOS values of the aortic media were calculated from at least five images

207 per case using the SAM manufacturer and commercial statistics software

208 (Statcel3-Addin forms on Excel, OMS publishing, Tokorozawa, Saitama, Japan), which

209 calculates the average areas-of-interest values. To detect the correlations between age

210 and SOS values and between age and MDG scores, scatter plots were established and

211 subjected to simple linear regression analysis. The correlation strength was quantified

212   using Pearson's correlation coefficients (r). The average SOS ($\pm$ SD) values from

213   younger and older aortae and between dissected aortae and age-matched normal aortae

214   were compared using unpaired Student's t-tests. The average SOS values ($\pm$ SD) among

215   different time points after collagenase were compared using paired t-tests.

216   It was confirmed that each data set followed a normal distribution pattern before

217   statistical analyses were conducted. Significance level for all tests was set at $p < 0.05$.

218

219   **Results**

220   ***Age-dependent changes in SOS and MDG of normal aortic media***

221   SOS values of the normal aortic media without calcified deposits and heavy atheroma

222   potions decreased with age (Fig. 2a). SOS values were negatively correlated with age (y

223     $= -0.6032x + 1699.3$, $r = -0.39$, $p = 0.015$).

224   The significantly positive relationship between age and MDG scores ($y =$

225     $0.021x + 0.21$, $r = 0.56$, $p = 0.0003$) is shown in Figure 2b. **The significantly negative**

226   **relationship between SOS and MDG scores ($y = -0.012x + 22.47$, $r = -0.505$, $p =$**

227   **0.0016) is shown in Figure 2c.**

228

229   ***Relationship between age and SOS or MDG of dissected aortae***

230 **SOS values and MDG scores of dissected aortae were compared with those of**

231 **age-matched normal ones (Fig. 2d).** The dissection group exhibited significantly

232 greater SOS values ($p = 8.50E\text{-}10$) and higher MDG scores ($p = 0.043$) than the normal

233 group. No significant correlation between age and SOS values ($y = -0.2334x + 1738$, r

234 $= -0.17$, $p = 0.501$) (Fig. 2a) or age and MDG scores ($y = 0.0025x + 1.83$, $r = 0.075$, p

235 $= 0.772$) (Fig. 2b) was observed in dissected aortae. **There was also no significant**

236 **relationship between SOS value and MDG scores ($y = -0.0054x + 11.45$, $r = -0.21$, p**

237 **$= 0.42$) (Fig. 2c).**

238

239 *Differential changes in SOS values between older and younger aortae after*

240 *collagenase digestion*

241 Before collagenase digestion, the older aortic media (n = 22) showed significantly lower

242 SOS values than the younger aortae (n = 20) (Figs. 3a and 3b; Table A1). After

243 collagenase digestion, both older and younger aortae showed lower SOS values. At 1.5

244 h after digestion, SOS values significantly decreased in both cases ($p < 0.01$) (Fig. 4).

245 EMT staining revealed wavy, thin, and split elastic fibers in the media from the older

246 aorta, whereas the younger aortae contained thicker and straighter fibers. LM images

247 obtained 3 h after digestion revealed numerous fragmented elastic fibers in the older

248   aortae compared to the younger aortae. Similar to the baseline difference at 0 h, older

249   aortae had significantly lower SOS values than younger aortae after 1.5 h and 3 h of

250   collagenase digestion (p's < 0.01).

251

252   ***Differential changes in SOS values between dissected aortae (MF and non-MF***

253   ***syndrome) and normal aortae after collagenase digestion***

254   Cases of dissected aortae with MF had cystic mucoid degeneration and elastic fiber

255   fragmentation or loss. Cystic degeneration displayed low SOS values (Fig. 3c). Non-MF

256   cases consisting of thick parallel muscles and wavy elastic fibers with focal splitting

257   showed high SOS values (Fig. 3d). SOS values decreased faster after digestion in cases

258   of dissected aortae compared to age-matched controls (Fig. 4 and Table A2). At baseline,

259   the two groups showed significantly different SOS values ($p = 0.0001$). However, the

260   difference in SOS values disappeared after 1.5 h ($p = 0.100$) and 3 h ($p = 0.346$). In

261   contrast to the SOS results, LM images in EMT staining showed no major differences

262   between MF syndrome and non-MF syndrome cases. There was slight muscle fiber

263   disappearance and loose elastic fibers before and after digestion.

264

265   ***Structure components of SMA, collagen type-I, and collagen type-III in the older,***

266   *younger, MF, and non-MF aortae*

267   Regarding SMA immunostaining (Fig. 5a), old aortae showed focal loss of smooth

268   muscles, whereas younger aortae consisted of continuous parallel muscles. MF cases

269   displayed aggregated muscle fibers with irregular arrangement, whereas non-MF cases

270   showed scattered loss of smooth muscle fibers.

271   Regarding collagen type-I (Fig. 5b) and type-III (Fig. 5c), normal young and

272   old cases displayed parallel collagen fibers. Non-MF cases had rich collagen fibers,

273   although fiber arrangement was irregular. MF cases had poor collagen fibers with

274   irregular arrangement among cells. Table 1 details the immunohistochemical results.

275

276   ***ECM components of LOX, VN, FBN, and FN in the younger, older, MF, and non-MF***

277   ***aortae***

278   Immunostaining with anti-LOX (Fig. 6a) showed that normal younger and older aortae

279   exhibited no to faint positive staining. However, the MF aortae revealed strong

280   punctate-patterned staining on smooth muscles, whereas the non-MF aortae showed

281   weak positive staining.

282   Regarding the VN (Fig. 6b), all normal young or old aortae and MF and

283   non-MF ones were focally positive, although MF cases showed a rather irregular

16

284   distribution.

285   About FBN (Fig. 6c), all cases except MF were positive. Concerning FN (Fig.

286   6d), old and non-MF cases were positively associated with muscle fibers, whereas

287   young and MF aortae exhibited negative or focal weak positivity.

288

289

290   **Discussion**

291   Both structural and mechanical alterations in AAo were found with aging and dissection

292   cases using SAM combined with collagenase treatment and immunostaining. Age was

293   negatively correlated with SOS values based on SAM results, suggesting that the

294   non-atheromatous or calcified portions of the aorta become mechanically weaker with

295   age. In general, aging aortic walls show an increased stiffness due to atherosclerosis and

296   calcification. However, non-atheromatous portions of media showed loose and irregular

297   arrangement of smooth muscles and collagen fibers, which contributed to aneurysms

298   and rupture. **The MDG scores that increased with aging were significantly**

299   **negatively correlated with SOS values of non-atheromatous portions. The dissected**

300   **aortae cases, in which SOS values and MDG scores were both higher than those of**

301   **their age-matched controls, showed no significant alteration with aging.** This may

302 indicate that dissected aortic walls have greater stiffness to compensate for structural

303 defects, but are focally fragile and prone to ruptures. The susceptibility to collagenase

304 digestion supported this speculation. Other risk factors for dissection apart from aging

305 must also be present, such as genetic susceptibility. Not only MF syndrome cases but

306 also non-MF young cases may present genetic defects of ECM components.

307   Regarding damage caused by collagenases, both young and older cases

308 exhibited significantly decreased SOS values following 1.5 h and 3 h of collagenase

309 treatment. Young aortae retained rather high SOS values even after 3 h, whereas older

310 aortae reached minimum values close to the risk threshold of rupture. At 3 h, the old

311 aortae were composed of loose filamentous fibers. The dissected aortae group, including

312 MF and non-MF cases, had very high SOS values at baseline and more rapidly

313 decreased values after 1.5 h and 3 h as compared to their age-matched controls.

314 **Dissected aortae may have greater stiffness due to compensation for structural**

315 **defects. Sufficient number of structural components offset fragile quality, as seen**

316 **in smooth muscle bundles of MF cases and rich collagen type-III fibers of non-MF**

317 **cases.**

318   The fibrous portions of the dissected aortae had consistent SOS values,

319 whereas the non-fibrous portions were more sensitive to enzymatic damages. Busuttil et

320   al. (1980) reported that collagenase activity is detected in the aneurysmal wall of

321   abdominal aorta. Therefore, positive results for collagenase testing may predict future

322   rupture.

323   Immunostaining of the structural fibers in young aortae showed a continuous

324   parallel array, while the structural fibers in the old aortae were divided or sparse.

325   Regarding ECM proteins, FN was enriched in the older aortae compared to the younger

326   aortae. In the dissected aortae, MF cases had irregular distribution of SMA, collagen I,

327   and collagen III fibers, whereas most non-MF cases had distribution that was similar to

328   the normal older aortae. MF cases were positive for LOX and VN antigens, although

329   FBN and FN immunostaining was negative or faint. Both non-MF and elderly cases

330   exhibited a similar pattern of positivity for LOX, VN, FBN, and FN.

331   The histopathological alterations in dissection cases include smooth muscle cell

332   disappearance, medial mucoid degeneration, and ECM breakdown (Michel et al. 2018;

333   Wu et al. 2013). Dissection is performed because of genetic causes or degeneration with

334   aging (Michel et al. 2018). Among the 29 thoracic dissected aortae-associated genes

335   identified to date, the majority encode proteins involved in the extracellular matrix,

336   smooth muscle cell contraction or metabolism, or transformation of the growth factor-β

337   signaling pathway (Brownstein et al. 2017). SMA, collagens 1 and 3, elastin, FBN1, and

338   LOX are also included. MF syndrome, an autosomal dominant inherited disorder caused

339   by mutations in FBN1 (Dietz 1991), was reported to have increased expression of

340   matrix metalloproteinase (MMP)-2 and MMP-9 and premature aortic smooth muscle

341   cell differentiation (Dale et al. 2017).

342   Regarding ECM proteins, LOX is an extracellular amine oxidase that primarily

343   functions as a catalyst on the covalent cross-linking of collagen and elastin fibers in

344   ECM (Kagan and Li 2003). VN in ECM is involved in tissue repair and remodeling

345   (Leavesley et al. 2013). FBN-1 plays a crucial role in stabilizing the structure of elastic

346   fiber. FN plays roles in cell adhesion, migration, growth, and differentiation (Sottile

347   2002). FN in ECM controls deposition, organization, and stability of other matrix

348   proteins, including type-I collagen and type-III collagen. Specific types of ECM

349   proteins are expressed differently among MF, non-MF, and normal old cases to maintain

350   the mechanical strength of the aortic wall.

351   Although the resolution and flexibility in SAM imaging is not better than LM

352   imaging, it still has several advantages. First, no staining is required, which allows for

353   imaging of the sample within a few minutes. **Second, SOS values are digital, allowing**

354   **easy quantitative comparison among lesions.** Third, the virtual color images of SOS

355   values are adjustable based on the range of interest, facilitating easy detection of

356   abnormal regional alterations. Fourth, protease digestion alterations can be repeatedly

357   monitored with greater sensitivity compared to LM.

358   This study has several limitations that should be acknowledged. First, the

359   observed tissues were FFPE sections. Compared with fresh tissues, tissues fixed for

360   extended periods, such as those used for autopsies, become harder. However, the current

361   study reported SOS values in normal autopsy cases that were lower than those in

362   surgical specimens. The SOS values of fresh and formalin-fixed aortae have been

363   previously reported. Akhtar et al. (2016) reported that the SOS value of fresh aortae was

364   between 1,538 and 1,709 m/s. Saijo et al. (1998) reported SOS values of 1,614 ± 30 m/s

365   in formalin-fixed frozen sections of the aorta without paraffin-embedded treatment. Our

366   cases showed that the overall **mean** SOS value was 1,648.4 ± 30.2 m/s (age range, 16–

367   101 years), indicating that SOS values in the FFPE aortae were somewhat greater than

368   those in fresh-frozen aortae, but similar to those previously reported. Sasaki et al.

369   (1996) reported the influence of formalin fixation on the acoustic properties of the

370   normal kidney. No significant differences in acoustic parameters, including SOS values

371   or attenuation were observed. The second limitation is that sex differences were not

372   considered. The consecutive autopsy and surgical tissue samples used were

373   predominantly from men, with a few samples from younger women. Because fewer

374 younger and postmenopausal women present with similar vascular alterations as men

375 (Waddell et al. 2001), gender bias may be low. Third, the non-MF group included

376 different etiologies; therefore, LM images might be distinctly different in non-MF cases.

377 However, these non-MF cases had some common histological findings, such as an

378 intralamellar mucoid matrix and fragmentation or thinning of the elastic fibers, as

379 demonstrated in representative images. Despite these limitations, SAM analysis with

380 protease digestion is a useful method to evaluate mechanical weakness due to histology

381 features and to investigate the cause of rupture.

382 **In conclusion, SOS values appropriately reflected mechanical weakness**

383 **and degeneration with aging. Dissected aortae had higher SOS values irrespective**

384 **of high MDG scores. All normal and dissected aortae were vulnerable to**

385 **collagenase digestion. Old aortae first reached the lowest level of SOS, and**

386 **compared with normal aortae, dissected ones showed more susceptible to**

387 **collagenase digestion. Old and dissected aortae had different structural**

388 **components to protect against mechanical weakness of the thoracic aorta.**

389

390

399

400 **Conflict of interest**

401 None.

402

403 **References**

404 Akhtar R, Cruickshank JK, Zhao X, Derby B, Weber T. A pilot study of scanning

405 acoustic microscopy as a tool for measuring arterial stiffness in aortic biopsies.

406 Artery Res Elsevier Ltd 2016;13:1-5.

407 Azhari H. Appendix A: Typical Acoustic Properties of Tissues. Basics Biomed

408 Ultrasound Eng Wiley-IEEE Press 2010:pp. 313-314.

409 Bamber JC, Hill CR, King JA, Dunn F. Ultrasonic propagation through fixed and

410 unfixed tissues. Ultrasound Med Biol 1979;5:159-165.

411 Brooke BS, Karnik SK, Li DY. Extracellular matrix in vascular morphogenesis and

412 disease: structure versus signal. Trends Cell Biol Elsevier Current Trends

413 2003;13:51-56.

414 Brownstein AJ, Ziganshin BA, Kuivaniemi H, Body SC, Bale AE, Elefteriades JA.

415 Genes associated with thoracic aortic aneurysm and dissection-an update and

416 clinical implications. Aorta 2017;5:11-20.

417 Busuttil RW. Collagenase activity of the human aorta. Arch Surg 980;115:1373-1378.

418 Choke E, Cockerill G, Wilson WRW, Sayed S, Dawson J, Loftus I, Thompson MM. A

419 review of biological factors implicated in abdominal aortic aneurysm rupture. Eur.

420 J Vasc Endovasc Surg 2005;30:227-44.

421   Dale M, Fitzgerald MP, Liu Z, Meisinger T, Karpisek A, Purcell LN, Carson JS,

422   Harding P, Lang H, Koutakis P, Batra R, Mietus CJ, Casale G, Pipinos I, Baxter

423   BT, Xiong W. Premature aortic smooth muscle cell differentiation contributes to

424   matrix dysregulation in Marfan Syndrome. PLoS One 2017;12:1-18.

425   Dietz H et al. Marfan syndrome caused by a recurrent de novo missense mutation in the

426   fibrillin gene. Nature 1991;352:337-9.

427   Duck FA. Acoustic properties of tissue at ultrasonic frequencies. In: Duck FA, ed. Phys

428   Prop Tissues London: Academic Press, 1990. pp. 73-135.

429   Fromageau J, Lerouge S, Maurice RL, Soulez G, Cloutier G. Noninvasive vascular

430   ultrasound elastography applied to the characterization of experimental aneurysms

431   and follow-up after endovascular repair. Phys Med Biol 2008;53:6475-6490.

432   Halushka MK, Angelini A, Bartoloni G, Basso C, Batoroeva L, Bruneval P, Buja LM,

433   Butany J, d'Amati G, Fallon JT, Gallagher PJ, Gittenberger-de Groot AC, Gouveia

434   RH, Kholova I, Kelly KL, Leone O, Litovsky SH, Maleszewski JJ, Miller D V,

435   Mitchell RN, Preston SD, Pucci A, Radio SJ, Rodriguez ER, Sheppard MN, Stone

436   JR, Suvarna SK, Tan CD, Thiene G, Veinot JP, van der Wal AC. Consensus

437   statement on surgical pathology of the aorta from the Society for Cardiovascular

438   Pathology and the Association For European Cardiovascular Pathology: II.

439   Noninflammatory degenerative diseases - nomenclature and diagnostic criteria.

440   Cardiovasc Pathol 2016;25:247-257.

441   Hozumi N, Yamashita R, Lee CK, Nagao M, Kobayashi K, Saijo Y, Tanaka M, Tanaka

442   N, Ohtsuki S. Time-frequency analysis for pulse driven ultrasonic microscopy for

443   biological tissue characterization. Ultrasonics 2004. pp. 717-722.

444   Hughes DJ, Babbs CF, Geddes LA, Bourland JD. Measurements of Young's modulus

445   of elasticity of the canine aorta with ultrasound. Ultrason Imaging 1979;1:356-367.

446   Kagan HM, Li W. Lysyl oxidase: Properties, specificity, and biological roles inside and

447   outside of the cell. J Cell Biochem 2003;88:660-72

448   Leavesley DI, Kashyap AS, Croll T, Sivaramakrishnan M, Shokoohmand A, Hollier BG,

449   Upton Z. Vitronectin - Master controller or micromanager? IUBMB Life

450   2013;65:807-818.

451   Lehmann ED, Parker JR, Hopkins KD, Taylor MG, Gosling RG. Validation and

452   reproducibility of pressure-corrected aortic distensibility measurements using

453   pulse-wave-velocity Doppler ultrasound. J Biomed Eng 1993;15:221-228.

454   Lemons RA, Quate CF. Acoustic microscope - Scanning version. Appl Phys Lett

455   1974;24(4):163-5.

456   Lemor RM, Weiss EC, Pilarczyk G, Zinin P V. Mechanical properties of single cells:

457   Measurement possibilities using time-resolved scanning acoustic microscopy. Proc

458   - IEEE Ultrason Symp 2004.

459 Maev RG. Acoustic properties of biological tissues and their effect on the image

460   contrast. Acoust Microsc Weinheim, Germany: Wiley-VCH, 2008. pp. 212-231.

461 Mahmood B, Ewertsen C, Carlsen J, Nielsen M. Ultrasound vascular elastography as a

462   tool for assessing atherosclerotic plaques - A systematic literature review.

463   Ultrasound Int Open 2016;02:E106-E112.

464 Mamou J, Rohrbach D. Image formation methods in quantitative acoustic microscopy

465   Jonathan Mamou and Daniel Rohrbach F . L . Lizzi Center for Biomedical

466   Engineering Riverside Research New York , NY , USA. IEEE Int Conf Acoust

467   Speech, Signal Process 2017;6259-6263.

468 Menashi S, Campa JS, Greenhalgh RM, Powell JT. Collagen in abdominal aortic

469   aneurysm: Typing, content, and degradation. J Vasc Surg 1987;6:578-582.

470 Michel J, Jondeau G, Milewicz DM. From genetics to response to injury : vascular

471   smooth muscle cells in aneurysms and dissections of the ascending aorta.

472   Cardiovasc Res 2018;578-589.

473 Miura K. Application of scanning acoustic microscopy to pathological diagnosis. In:

474   Stanciu SG, ed. Microsc Anal Croatia: Intech, 2016. pp. 381-403.

475   Miura K, Egawa Y, Moriki T, Mineta H, Harada H, Baba S, Yamamoto S. Microscopic

476   observation of chemical modification in sections using scanning acoustic

477   microscopy. Pathol Int 2015;65:355-366.

478   Miura K, Katoh H. Structural and histochemical alterations in the aortic valves of

479   elderly patients: A comparative study of aortic stenosis, aortic regurgitation, and

480   normal valves. Biomed Res Int 2016;2016.

481   Miura K, Yamamoto S. A scanning acoustic microscope discriminates cancer cells in

482   fluid. Sci Rep 2015;5.

483   Radu-Ionita F, Ţintoiu IC, Rosu A, Bontas E, Cochior D, Bolohan R, Silvestru C, Ifrim

484   M, Mocanu I, Riga D, Murgu V, Riga S, Savoiu D, Kibos A. Aging aorta-cellular

485   mechanisms. New Approaches to Aortic Dis from Valve to Abdom Bifurc

486   2017;3-23.

487   Saijo Y. Acoustic microscopy: latest developments and applications. Imaging Med

488   London: Future Medicine Ltd 2009;1:47-63.

489   Saijo Y, Sasaki H, Okawai H, Nitta S, Tanaka M. Acoustic properties of atherosclerosis

490   of human aorta obtained with high-frequency ultrasound. Ultrasound Med Biol

491   1998;24:1061-1064.

492   Sasaki H, Saijo Y, Tanaka M, Okawai H, Terasawa Y, Yambe T, Nitta SI. Influence of

493   tissue preparation on the high-frequency acoustic properties of normal kidney

494   tissue. Ultrasound Med Biol 1996;22:1261-1265.

495   Schmitt C, Hadj Henni A, Cloutier G. Ultrasound dynamic micro-elastography applied

496   to the viscoelastic characterization of soft tissues and arterial walls. Ultrasound

497   Med Biol 2010;36:1492-1503.

498   Sottile J. Fibronectin polymerization regulates the composition and stability of

499   extracellular matrix fibrils and cell-matrix adhesions. Mol Biol Cell

500   2002;13:3546-3559.

501   Sutton-Tyrrell K, Najjar SS, Boudreau RM, Venkitachalam L, Kupelian V, Simonsick

502   EM, Havlik R, Lakatta EG, Spurgeon H, Kritchevsky S, Pahor M, Bauer D,

503   Newman A. Elevated aortic pulse wave velocity, a marker of arterial stiffness,

504   predicts cardiovascular events in well-functioning older adults. Circulation

505   2005;111:3384-3390.

506   Tsamis A, Krawiec JT, Vorp DA. Elastin and collagen fibre microstructure of the

507   human aorta in ageing and disease: a review. J R Soc Interface 2013;10:20121004.

508   Waddell TK, Dart AM, Gatzka CD, Cameron JD, Kingwell BA. Women exhibit a

509   greater age-related increase in proximal aortic stiffness than men. J Hypertens

510   2001;19:2205-2212.

511   Weiss EC, Anastasiadis P, Pilarczyk G, Lemor RM, Zinin P V. Mechanical properties

512   of single cells by high-frequency time-resolved acoustic microscopy. IEEE Trans

513   Ultrason Ferroelectr Freq Control 2007;54:2257-2271.

514   Wittek A, Karatolios K, Bihari P, Schmitz-Rixen T, Moosdorf R, Vogt S, Blase C. In

515   vivo determination of elastic properties of the human aorta based on 4D ultrasound

516   data. J Mech Behav Biomed Mater 2013.

517   Wu D, Shen YH, Russell L, Coselli JS, Lemaire SA. Molecular mechanisms of thoracic

518   aortic dissection. J. Surg. Res. 2013.

519

520

521

Figure captions

Fig. 1 Flow chart of SAM observation

Fig. 2 Relationship among age, **mean** speed-of-sound (SOS), and grade of medial

degeneration (MDG) in normal and dissected aortae

a. Relationship between average SOS value and age of normal and dissection aortae. b.

Relationship between MDG scores and age of normal and dissected aortae. **c.**

Relationship between SOS value and MDG scores. d. Boxplot showing the SOS and

MDG difference between normal and dissected cases. r = Peason's correlation

coefficient.

Fig. 3 Representative speed-of-sound (SOS) images of the aortae after collagenase

type-III digestion (a: 85-year-old woman, b: 31-year-old man, c: Marfan (MF)

syndrome, d: Non-MF syndrome)

SOS images exhibited gradual decreases in SOS values at 1.5 h and 3 h after digestion.

The corresponding light microscopy (LM) images of Elastica Masson trichrome (EMT)

staining before and after 3 h of collagenase digestion are shown in the upper rows. The

elderly aorta (b) appears with more fragmentation of elastic fibers. The aortae in both

541   MF (c) and non-MF (d) cases exhibit rapidly decreasing SOS values after collagenase

542   digestion. The MF case with cystic mucoid degeneration shows punctate low SOS areas

543   on the right side. The non-MF aorta consisting of parallel muscle fibers and wavy

544   elastic fibers with focal splitting shows high SOS at the baseline. Black bar = 400 μm,

545   red bar = 10 μm.

546

547   **Fig. 4** Reduction of SOS after collagenase digestion (left: young and old, right:

548   dissection and age-matched normal controls)

549   SOS of all groups decreased from 0 to 1.5 h, and 1.5 h to 3 h after collagenase digestion.

550   SOS values in dissection cases decreased more rapidly than those in normal

551   age-matched aortae. ***$p < 0.001$, **$p < 0.01$, *$p < 0.05$.

552

553   **Fig. 5** Immunostaining with anti-smooth muscle actin (SMA) (a), anti-collagen type-I

554   (COL 1) (b), and anti-collagen type-III (COL 3) (c) antibodies of young, elderly, MF,

555   and non-MF sections

556   Regarding the SMA, the young aortae showed parallel linear smooth muscles, whereas

557   the old aortae exhibited split smooth muscle fibers. MF cases displayed aggregated

558   SMA bundles with irregular arrangement, whereas non-MF cases showed frayed muscle

559   fibers with irregular arrangement. Regarding COL 1 and COL 3, young and elderly

560   cases displayed parallel fiber components between smooth muscle fibers, although the

561   fiber array was irregular in old cases. MF cases had irregular fiber arrangements among

562   cells, whereas non-MF cases exhibited rich collagen fibers in a focal irregular array.

563

564   **Fig. 6** Immunostaining with anti-lysyl oxidase (LOX) (a), vitronectin (VN) (b), fibrillin

565   (FBN) (c), and fibronectin (FN) (d) antibodies of young, elderly, MF, and non-MF

566   sections

567   The normal young aorta was negative for LOX, whereas the old aorta showed focal

568   faint positivity. MF aortae exhibited strong punctate positivity on smooth muscles for

569   LOX, whereas non-MF aortae showed focal weak positivity. In VN, all normal young or

570   old aortae and MF and non-MF aortae, displayed focal positivity, although MF cases

571   show rather irregular distribution. For FBN, only MF cases exhibited negative. For FN,

572   old and non-MF cases show positivity along muscle fibers.

573

Fig. 1

Autopsy or Surgical specimen of aortae

10% buffered formalin fix

↓

Vertical cut aortae

↓   ↘

10-µm flat section   LM sample

↓

Obtain SAM image, use distilled water as coupling medium

↓

Calculate average SOS values of media except calcification and severe atherosclerosis
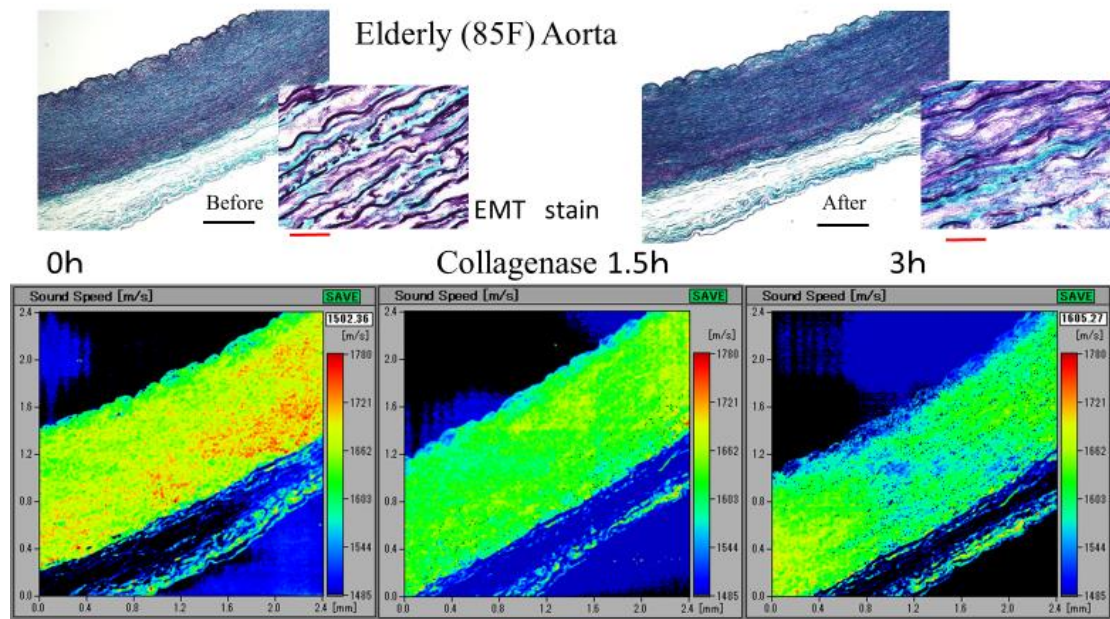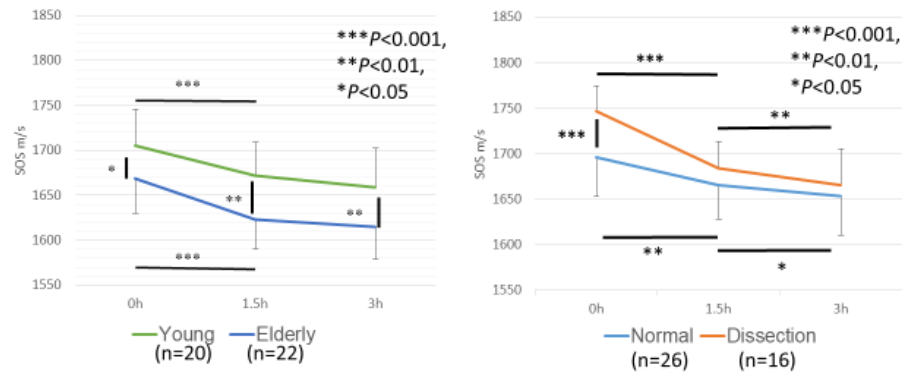
↓

Collagenase digestion if necessary

↓

Time-lapse observation of the same section

Fig. 2a

Fig. 2b

Fig. 2c

Fig. 2d

Fig. 3a

Elderly (85F) Aorta

Before   EMT stain   After

0h   Collagenase 1.5h   3h

Fig. 3b

Young (31M) Aorta

EMT stain

Before · After

0h · Collagenase 1.5h · 3h

Fig. 3c

Marfan Ao
with dissection

EMT stain

0h   Collagenase 1.5h   3h

Fig. 3d

Non-Marfan Ao with dissection

◁ Dissected space

EMT stain

Before

After

0h   Collagenase 1.5h   3h
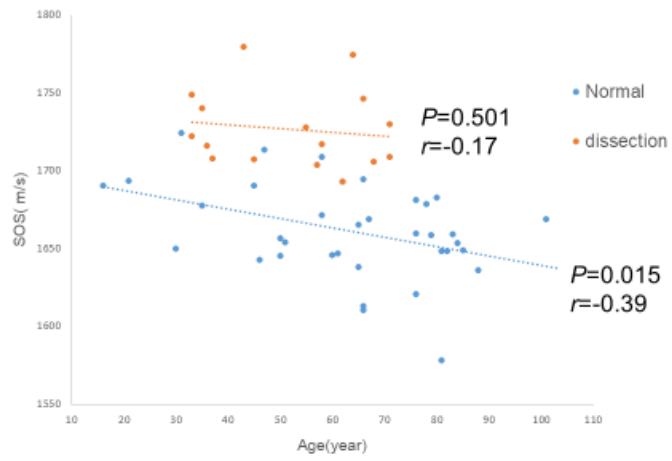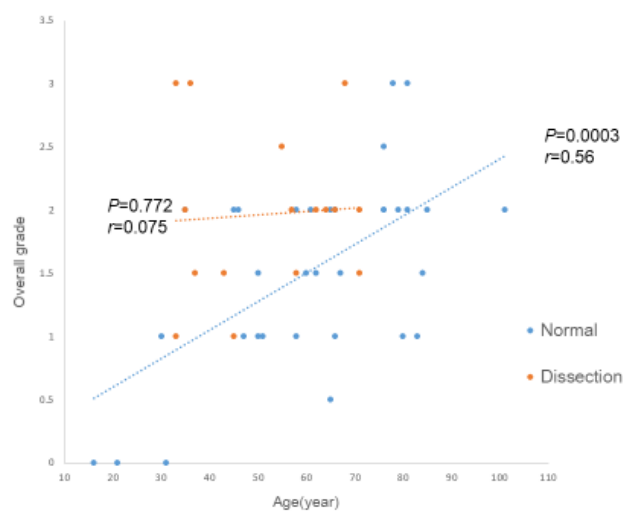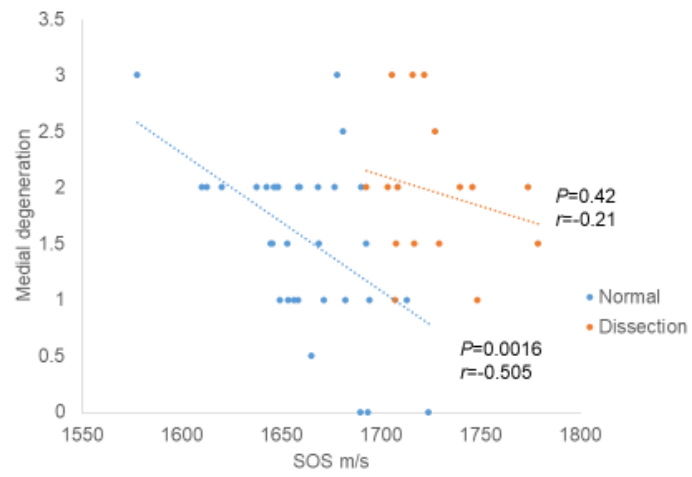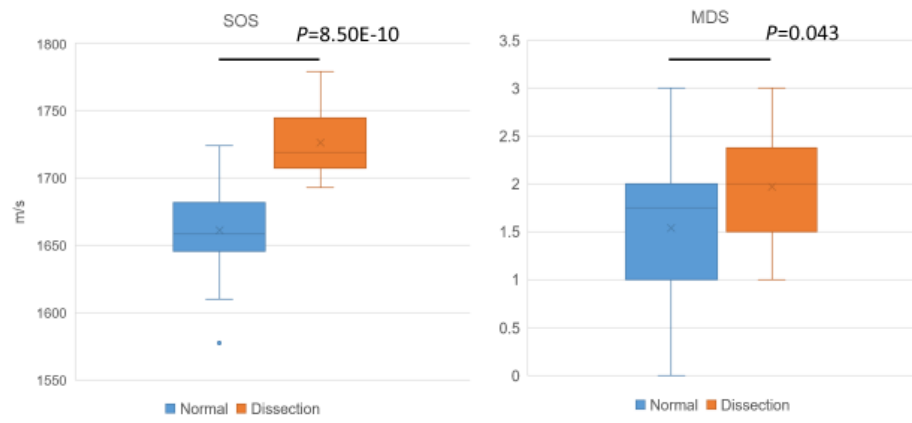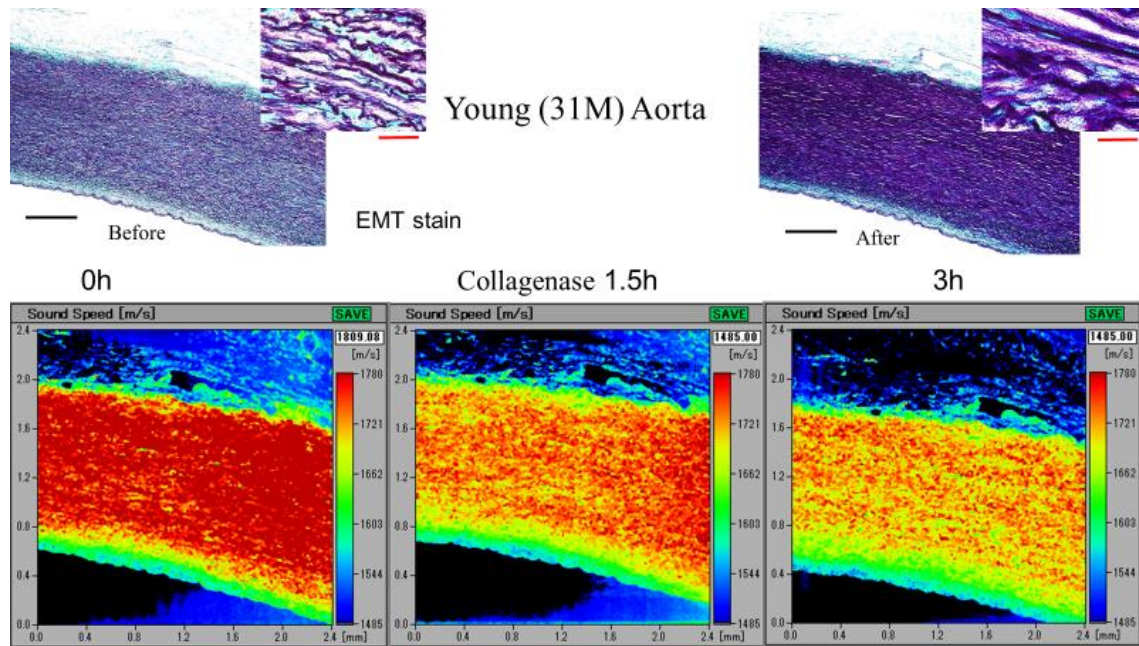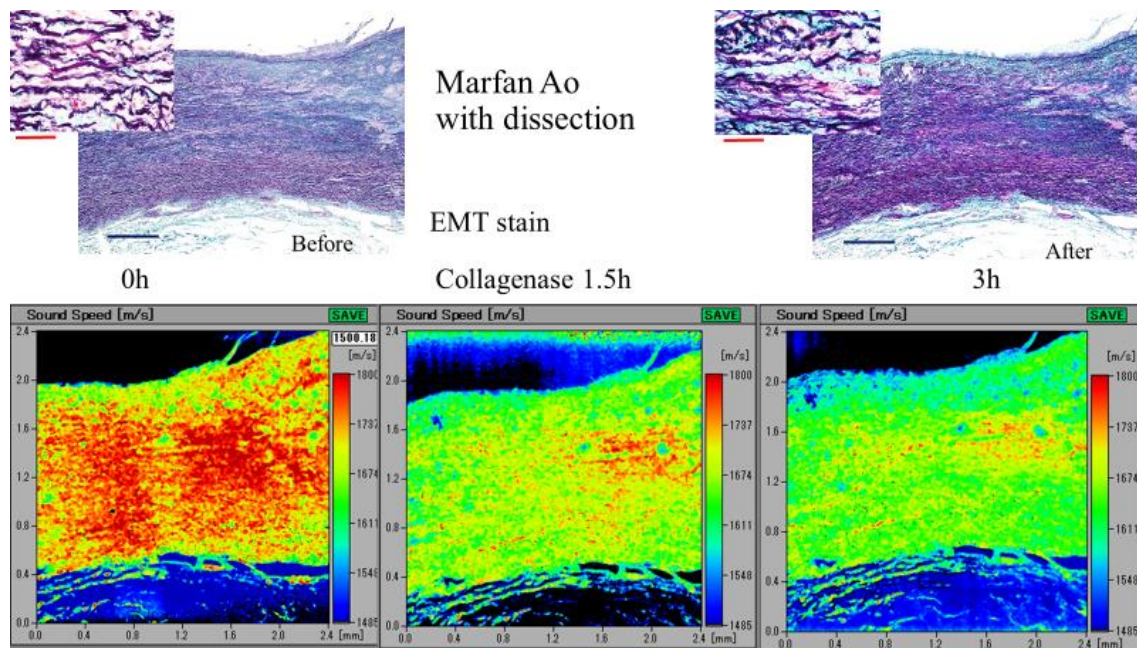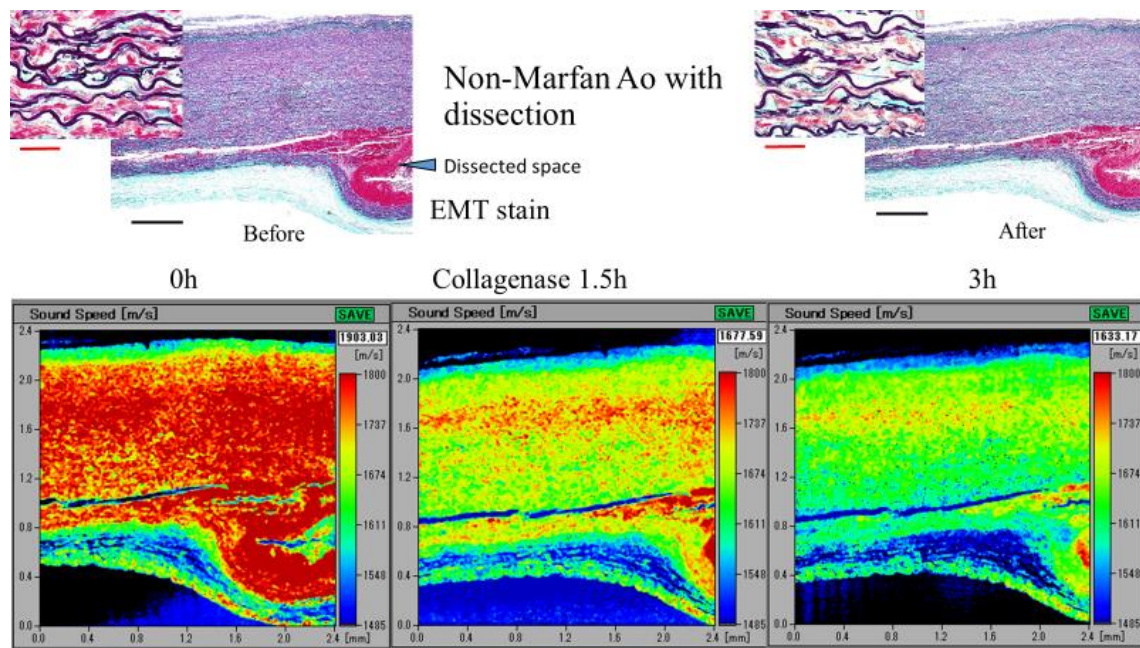
Fig. 4

Fig. 5a
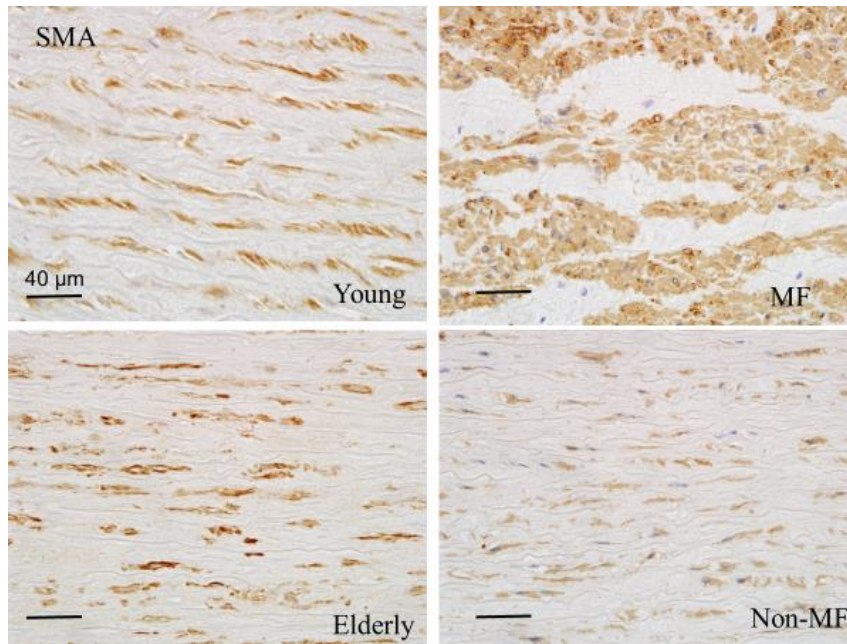
Fig. 5b
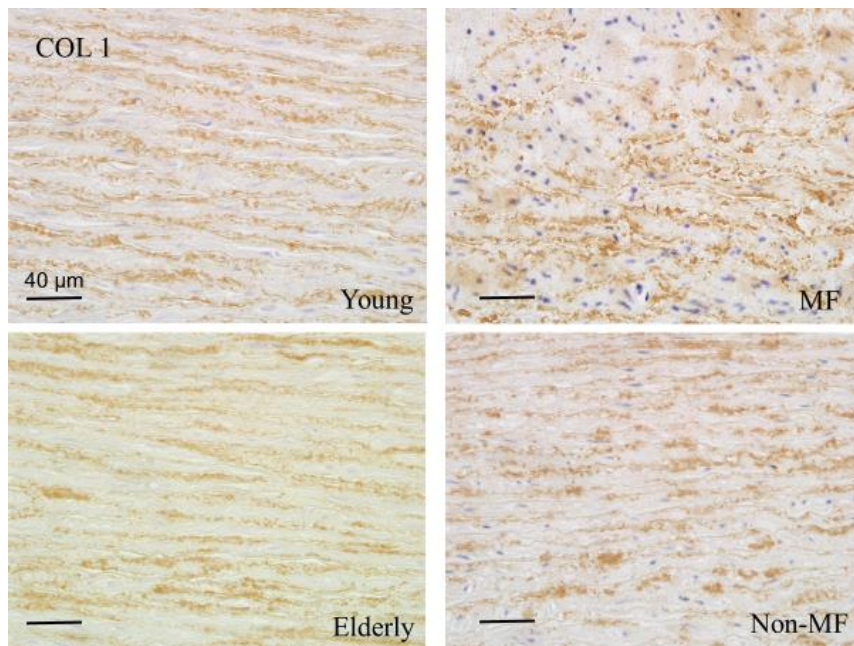
Fig. 5c
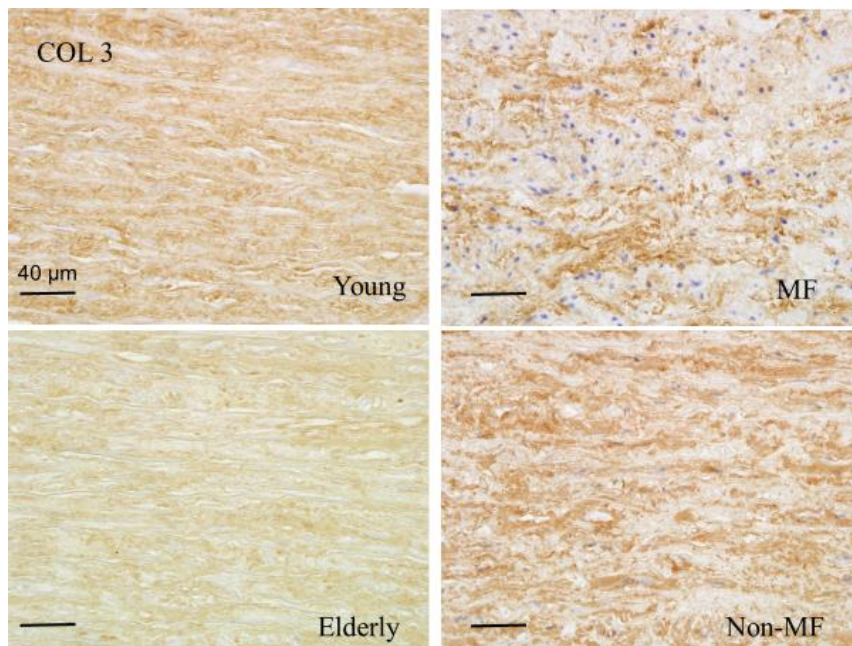
Fig. 6a
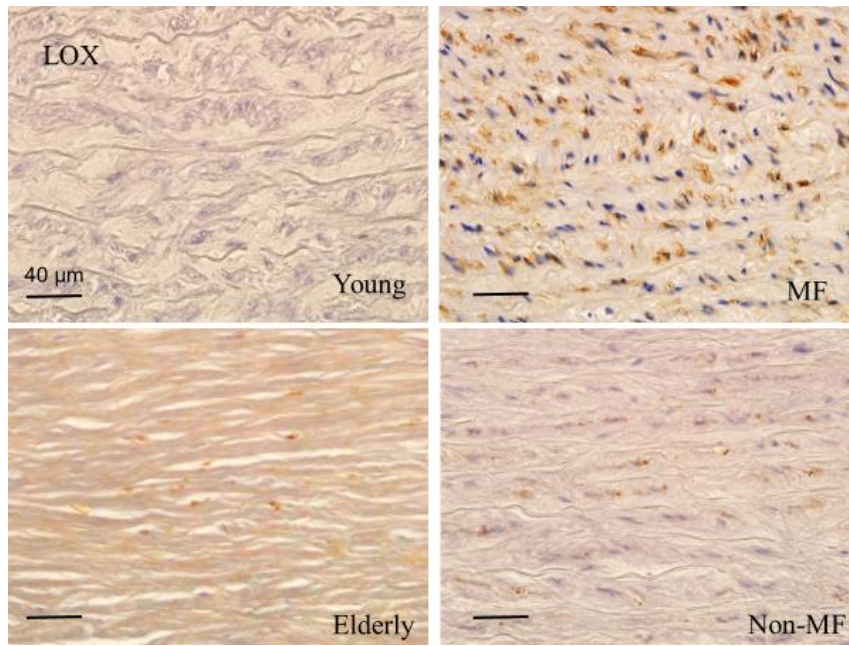
Fig. 6b
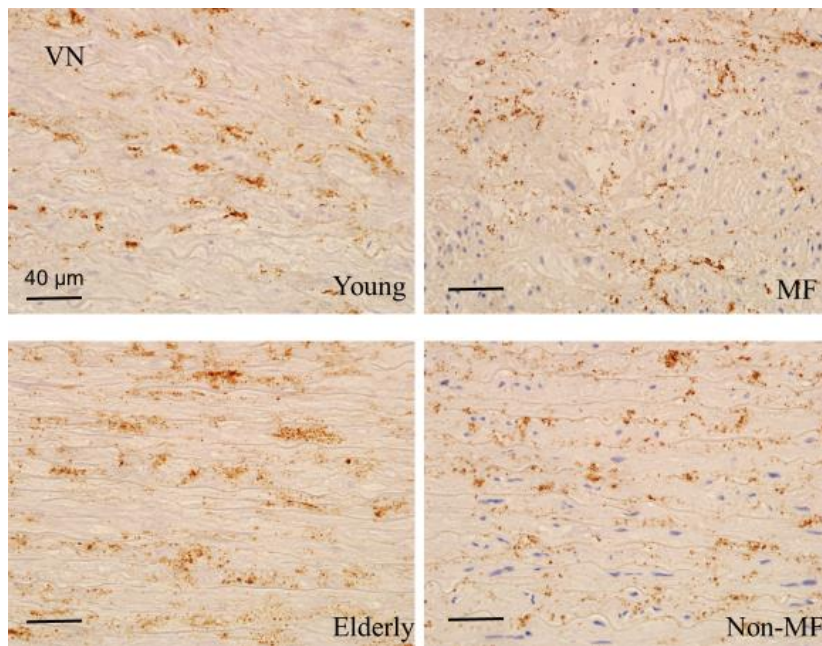
Fig. 6c
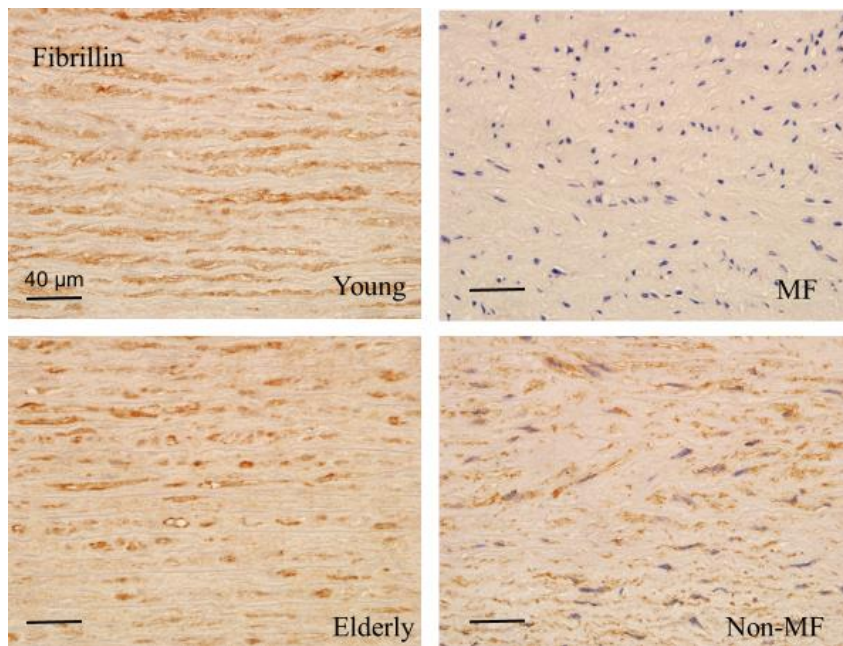
Fig. 6d
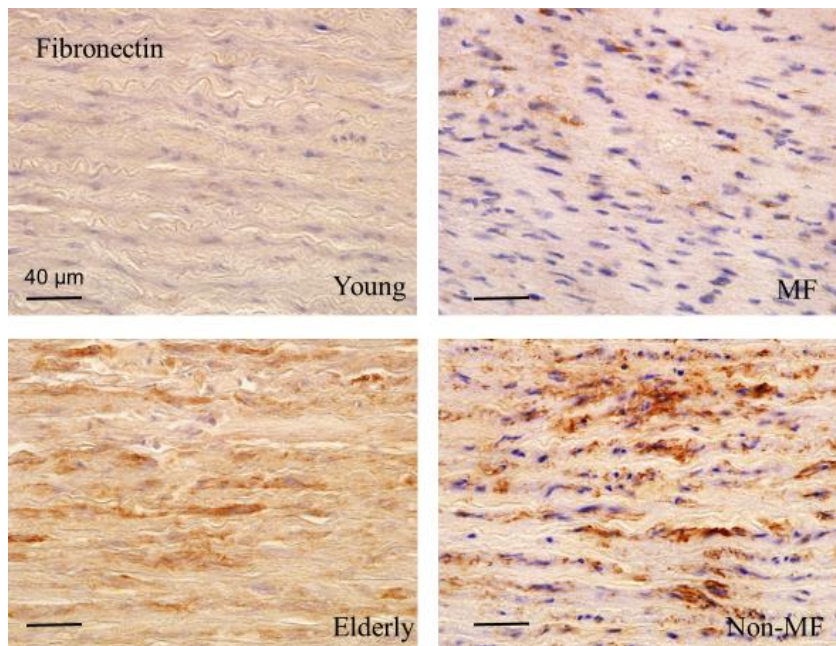
Table

Table 1. Immunostaining results of the supporting components

Case	SMA	Col 1	Col 3	LOX	VN	FBN	FN
N-Young	+	+	+	−	+	+	−
N-Old	+F,W	+F,W	+	+W	+F	+	+
MF	+F	+F	+F	++	+	−	+F,W
Non-MF	+F,W	+F,W	+F,W	+F	+	+	+

N-Young, normal young; N-Old, normal old; MF, Marfan syndrome; F, focal; W, weak;

SMA, smooth muscle actin; Col 1, collagen type-I; Col 3, collagen type-III; LOX, lysyl

oxidase; VN, vitronectin; FBN, fibrillin; FN, fibronectin

Table A.1. Average speed-of-sound (SOS) of older (OL) and younger (YG) aortae after

collagenase digestion

Collagenase	n	Average	SD
		m/s	
YG0h	20	1705.1	40.6
YG1.5h	20	1672.3	36.7
YG3h	20	1658.8	43.5
OL0h	22	1668.4	38.1
OL1.5h	22	1622.7	32.9
OL3h	22	1614.5	36.0

*** $p < 0.001$. **$p < 0.01$, *$p < 0.05$

1   Table A.2. Average speed-of-sound (SOS) of normal (NOR) and dissection (DIS) aortae

2   after collagenase digestion.

Collagenase	n	Average m/s	SD
0h-NOR	26	1695.8	42.5
1.5h-NOR	26	1665.6	37.7
3h-NOR	26	1653.3	42.5
0h-DIS	16	1741.1	27.6
1.5h-DIS	16	1684.0	29.0
3h-DIS	16	1665.8	39.3

**   *   ***   ***   ***

3   *** $p < 0.001$, **$p < 0.01$, *$p < 0.05$

4